Can Donor Ligands Make Pd(OAc)₂ a Stronger Oxidant?

Access to Elusive Palladium(II) Reduction Potentials and Effects of

Ancillary Ligands via Palladium(II)/Hydroquinone Redox Equilibria

David L. Bruns, † Djamaladdin G. Musaev‡, Shannon S. Stahl*†

[†] Department of Chemistry, University of Wisconsin-Madison, 1101 University Avenue Madison, WI, 53706, United States

[‡] Cherry L. Emerson Center for Scientific Computation and Department of Chemistry, Emory University, Atlanta, Georgia 30322, United States

Abstract: Palladium(II)-catalyzed oxidation reactions represent an important class of methods for selective modification and functionalization of organic molecules. This field has benefitted greatly from the discovery of ancillary ligands that expand the scope, reactivity, and selectivity in these reactions; however, ancillary ligands also commonly poison these reactions. The different influences of ligands in these reactions remain poorly understood. For example, over the 60-year history of this field, the Pd^{II/0} redox potentials for catalytically relevant Pd complexes have never been determined. Here, we report the unexpected discovery of (L)Pd^{II}(OAc)₂-mediated oxidation hydroquinones, the microscopic reverse of quinone-mediated oxidation of Pd⁰ commonly employed in Pd^{II}-catalyzed oxidation reactions. Analysis of redox equilibria arising from the reaction of (L)Pd(OAc)₂ and hydroquinones (L = bathocuproine, 4,5-diazafluoren-9-one), generating reduced (L)Pd species and benzoquinones, provides the basis for determination of (L)Pd^{II}(OAc)₂ reduction potentials. Experimental results are complemented by density functional theory calculations to show how a series of nitrogen-based ligands modulate the (L)Pd^{II}(OAc)₂

reduction potential, thereby tuning the ability of Pd^{II} to serve as an effective oxidant of organic molecules in catalytic reactions.

Introduction

The field of homogeneous palladium catalyzed reactions for organic synthesis originated in 1959 with the discovery of the Wacker process, which features palladium(II)-catalyzed oxidative coupling of ethylene and water to generate acetaldehyde. Subsequent research efforts led to the discovery of numerous other oxidation reactions, including Wacker-type oxidative coupling of alkenes with diverse heteroatom and carbon-based nucleophiles; oxidative 1,4-difunctionalization of conjugated dienes; aromatic and allylic C–H oxidation reactions, including oxidative biaryl coupling, Fujiwara-Moritani coupling of arenes and alkenes, and allylic acetoxylation. These reactions typically employed palladium(II) catalysts with a stoichiometric oxidant to support reoxidation of Pdo to Pd

Scheme 1. Role of Benzoquinone as a (Co-)Oxidant in Palladium-Catalyzed Oxidation Reactions

$$H_2O$$
 $Co-Cat^{red}$
 H_2O
 H_2O

Catalysts used during the first several decades of this field primarily consisted of palladium(II) salts dissolved in polar solvents, but more recent efforts have emphasized ligand-supported catalysts. Oxidatively stable nitrogen donors, such as pyridine and phenanthroline, are among the most common class of ancillary ligands, but other examples include tertiary amines, sulfoxides, and *N*-heterocyclic carbenes. Ancillary ligands can impart multiple benefits to these reactions, including (1) facilitating catalyst turnover with O₂ rather than other stoichiometric oxidants, often without the need for redox co-catalysts; (2) enhancing catalyst stability by inhibiting decomposition of Pd⁰ into inactive nanoparticles or heterogeneous Pd; and (3) modulating chemo-, regio-, and stereoselectivity in synthetic oxidation reactions of alcohols, alkenes, C–H bonds, and other functional groups.¹⁸

Ancillary ligands play a crucial role in many homogeneous catalytic reactions; however, their use in Pd-catalyzed homogeneous oxidation reactions is somewhat paradoxical. Pd^{II} is the primary oxidant of the organic substrate, and coordination of electron-donating ligands to Pd^{II} is expected to make Pd^{II} a weaker oxidant. This consideration could explain why "ligand-free" catalyst systems dominated much of the early literature and synthetic applications within the field. Even in recent studies, ancillary donor ligands are commonly found to inhibit catalyst turnover. $^{19-23}$ Yet, direct insights into the influence of ligands on $Pd^{II/0}$ redox potentials are almost entirely lacking, and ligand selection is largely guided by intuitive concepts and empirical screening. Catalytically relevant Pd^{II} complexes, such as $(L)PdX_2$ species (L = bidentate ancillary donor ligand or two monodentate ligands; <math>X = OAc, CI, or other anionic ligand), exhibit complex electrochemical behavior that complicates acquisition of such insights. $^{24-27}$ Cyclic voltammetry studies yield irreversible waves arising from the different coordination environments of the corresponding Pd^{II}

and Pd⁰ species and/or from the formation of metastable species via one-electron redox steps and, therefore, the data do not provide reliable thermodynamic information.²⁸

Here, we present the first analysis of ligand effects on Pd^{II/0} redox potentials for (L)Pd(OAc)₂ complexes, using prototypical nitrogen-donor ligands commonly employed in Pd-catalyzed oxidation reactions. These ligands include pyridine (py), 2,2'-bipyridine (bpy), 1,10-phenanthroline (phen), bathophenanthroline (bphen; 4,7-diphenyl-1,10-phenantholine), 6,6'-dimethyl-2,2'-bipyridine (dmbpy), 2,9-dimethyl-1,10-phenantholine (dmphen), bathocuproine (bc; 2,9-dimethyl-4,7-diphenyl-1,10-phenanthroline), and 4,5-diazafluoren-9-one (DAF) (Figure 1). This study originates from an unexpected observation that certain ligated Pd(OAc)₂ complexes oxidize 1,4-hydroquinone (H₂BQ) to BQ, reversing the redox reaction featured in BQ-promoted Pd-catalyzed oxidation reactions (cf. Scheme 1). This reactivity provides the basis for unprecedented redox equilibria between palladium complexes and benzoquinone derivatives. Experimental and computational analysis of these reactions shows how the ancillary ligand structure modulates Pd^{II} redox potentials, sometimes in non-intuitive ways, and enables construction of a redox potential scale for the different (L)Pd(OAc)₂ complexes.

Figure 1. Representative ancillary nitrogen-based ligands encountered in Pd-catalyzed oxidation reactions and considered in the present study.

Results

In a 2010 study of Pd(OAc)₂-catalyzed allylic acetoxylation, we noted that DAF enabled good

Background context and discovery of (L)Pd(OAc)₂-mediated oxidation of hydroquinone.

reactivity with O₂ as the sole oxidant, ²⁹ while little or no catalytic turnover was observed with other ancillary nitrogen ligands (e.g., Figure 1). Beneficial effects of DAF have been noted in other Pd-catalyzed oxidation reactions. 23,30-40 and mechanistic studies highlight important ways in which DAF facilitates catalytic turnover, including its kinetic lability and access to multiple coordination modes. ^{23,29,41,42} In other reactions, ligands with methyl groups adjacent to the coordinating nitrogen atoms, including dmbpy, dmphen, and bc, have been shown to be effective. Mechanistic studies show that these ligands disfavor formation of inactive binuclear complexes^{43–} ⁴⁶ and undergo facile $\kappa^2 - \kappa^1$ interconversion to open coordination sites at the Pd^{II} center.²³ A factor not considered or investigated in these studies is the influence of the ancillary ligand on the Pd^{II/0} redox potential. Ligands that raise the reduction potential of Pd^{II} will increase the thermodynamic driving force for the substrate oxidation half-reaction and facilitate catalytic turnover (steps associated with substrate oxidation by Pd^{II} are often turnover limiting).¹⁸

An opportunity to probe the influence of ligands on the Pd^{II/0} redox potential arose unexpectedly from recent observations made while expanding on the synthetic utility of DAF/Pd(OAc)₂-catalyzed allylic oxidations.⁴⁷ We noted that benzoquinones could enhance the catalytic performance of DAF/Pd(OAc)₂, even in the absence of other redox active co-catalysts (cf. Scheme 1). This result suggested possible synergistic redox reactivity between Pd^{II} and BQ, including Pd^{II}-mediated oxidation of hydroquinone. 48-52 This possibility was not explored at the time, but provides the basis for the present investigation. A hydroquinone derivative, 2-tert-butyl-1,4-hydroquinone ('BuH₂BQ), was combined with DAF and Pd(OAc)₂ in dioxane:AcOH (3:1

vol:vol) under conditions resembling those used in the original study of DAF/Pd(OAc)₂-catalyzed allylic oxidation. The initial yellow-orange solution changed to deep-red upon standing at room temperature for several hours, and ¹H NMR analysis of the final products revealed the previously characterized Pd^I dimer, [Pd^I(μ-DAF)(OAc)]₂,^{42,53} and 2-*tert*-butyl-1,4-benzoquinone ('BuBQ). The 'BuBQ was obtained in 77% yield, when accounting for Pd as a one-electron oxidant (eq 1; see Supporting Information for details).

$$\begin{array}{c} 2 \text{ DAF/Pd(OAc)}_2 \\ \text{OH} \\ + \text{OH} \\ \end{array} \begin{array}{c} \text{OH} \\ \text{RT, 16 h, N}_2 \\ \text{OH} \\ \end{array} \begin{array}{c} \text{OAcO} \\ \text{N-Pd-N} \\ \text{OAc} \\ \text{OAc} \\ \end{array} \begin{array}{c} \text{OAc} \\ \text{77\%} \\ \text{OAc} \\ \end{array} \begin{array}{c} \text{OAc} \\ \text{OAc} \\ \text{OAc} \\ \text{OAc} \\ \end{array} \begin{array}{c} \text{OAc} \\ \text{OAc} \\$$

This result prompted us to test whether other ancillary ligands support the Pd^{II} -mediated oxidation of 'BuH₂BQ. Two different solvent systems, dioxane:acetic acid- d_4 (3:1) and chloroform- $d_1/1.5$ M acetic acid- d_4 , were used to account for differences in the solubility properties of the different Pd/ligand combinations and the use of dioxane and chlorinated solvents in the previous catalytic studies. ^{29,47} The reactions were conducted by adding 2 equiv of 'BuH₂BQ to solutions of L/Pd(OAc)₂ (L:Pd = 1:1 for bidentate ligands and 2:1 for pyridine) in the two solvent systems. The solutions were analyzed by ¹H NMR spectroscopy after 24 h at ambient temperature under N_2 (Figure 2A). In both solvents, very little 'BuH₂BQ conversion was observed in the absence of ancillary ligand and with py, bpy, phen, and bphen as ligands (< 10%), together with small amounts of Pd black. In dioxane/AcOD- d_4 , very low 'BuH₂BQ conversions were also observed with dmbpy, dmphen, and bc; however, 39% 'BuH₂BQ conversion was observed with DAF. No Pd black was observed in this reaction, and identification of [Pd^I(μ -DAF)(OAc)]₂ as the

reduced Pd product indicates that the 39% conversion corresponds to a 77% yield with respect to Pd^{II/I}, as noted above. In CDCl₃/AcOD-*d*₄, several ligands led to productive conversion of ${}^{t}BuH_{2}BQ$: dmbpy, dmphen, bc, and DAF led to ${}^{t}BuH_{2}BQ$ conversions of 41%, 36%, 16%, and

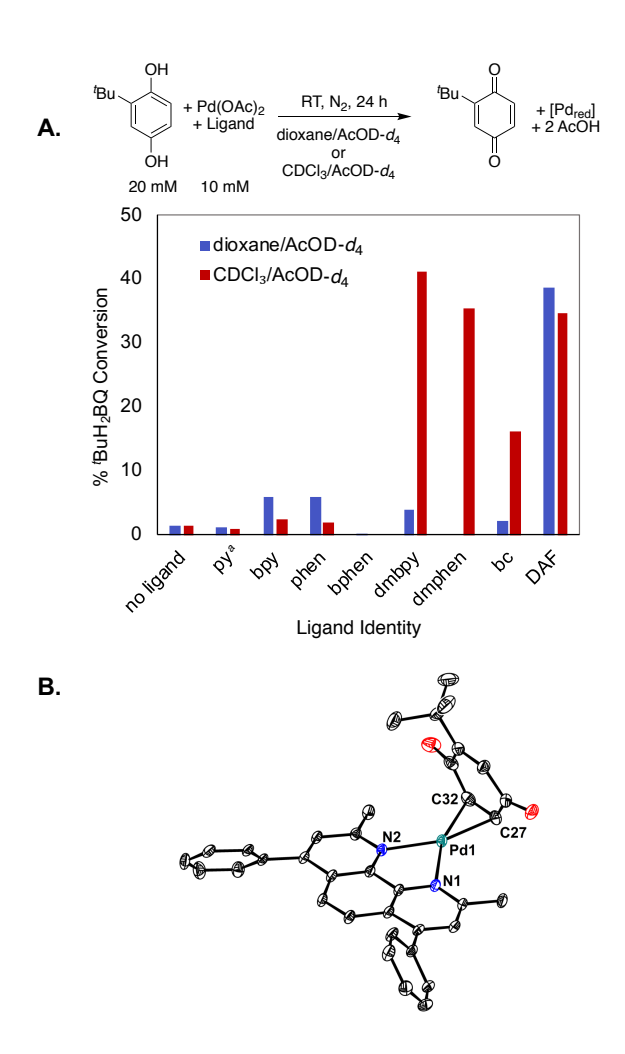


Figure 2. (A) Ligand effects on the Pd(OAc)₂-mediated oxidation of 'BuH₂BQ. Conversion determined by ¹H NMR spectroscopy using methyl-3,5-dinitrobenzoate (dioxane/AcOD-*d*₄) or 1,3,5-trimethoxybenzene (CDCl₃/AcOD-*d*₄) as an internal standard. ^a20 mM pyridine used. (B) X-ray crystal structure of (bc)Pd(^bBuBQ). H-atoms and solvent molecules omitted for clarity. See Section 9 of the Supporting Information for full details.

35%, respectively. All of these reaction solutions exhibited a color change, from yellow-orange to deep red. The red solution with DAF was attributed to the same Pd^I dimer observed in

dioxane:AcOH (cf. eq 1), although significant Pd black formation was also observed. Analysis of the products obtained from reactions with dmbpy, dmphen, and bc by ¹H NMR spectroscopy revealed four distinct resonances associated with the *tert*-butyl group and three ring protons for ¹BuBQ, but the peaks were shifted upfield relative to free ¹BuBQ. Crystals were obtained from the reaction of ¹BuH₂BQ and (bc)Pd(OAc)₂, and X-ray diffraction analysis revealed the identity of (bc)Pd(η^2 -¹BuBQ) as the product of the reaction (Figure 2B). ^{54–58} Similar species were evident in the ¹H NMR spectra with the dmbpy and dmphen ligands, but the products were less stable and led to relatively rapid Pd black formation. Consequently, subsequent studies focused on the reactions of DAF- and bc-ligated Pd complexes.

Characterization of redox equilibria between DAF/Pd(OAc)₂ and hydroquinones. The partial conversion observed in the reaction of 'BuH₂BQ and DAF/Pd(OAc)₂ described above raised the possibility that an equilibrium is established between the reagents and products. To explore this possibility, the reaction between 'BuH₂BQ and DAF/Pd(OAc)₂ was monitored by ¹H NMR spectroscopy. Only partial conversion to 'BuBQ and [Pd¹(μ-DAF)(OAc)]₂ (Figure 3A) was observed, and the same product mixture was obtained when the reverse reaction was analyzed, starting with independently prepared [Pd¹(μ-DAF)(OAc)]₂ and 'BuBQ (Figure 3B). These observations confirm equilibration between the oxidized and reduced Pd and quinone species, and the final concentrations indicate an equilibrium constant of 305 M for the reaction in eq 1, according to the expression in eq 2.

$$K_{eq} = \frac{[[Pd(\mu-DAF)(OAc)]_2] \cdot [^tBuBQ] \cdot [AcOH]^2}{[DAF/Pd(OAc)_2]^2 \cdot [^tBuH_2BQ]}$$
(2)

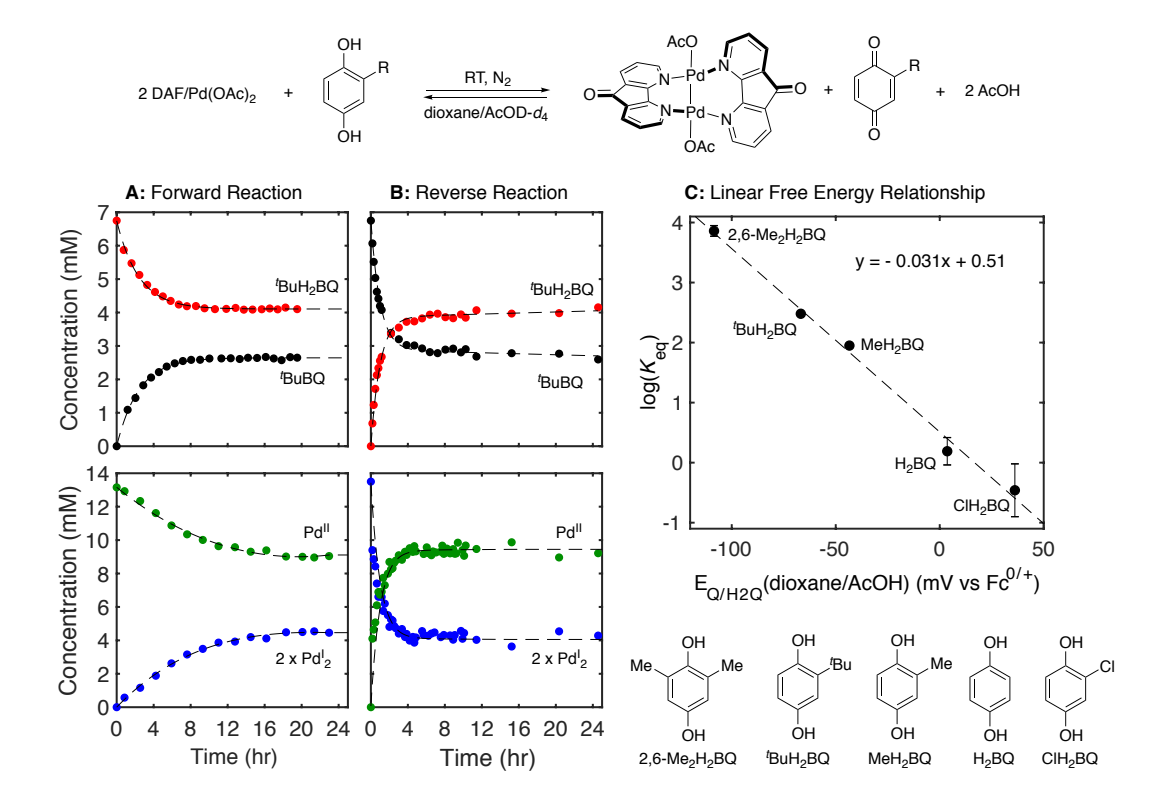


Figure 3. Approach-to-equilibrium concentration data. A: Forward Reaction: oxidation of tBuH_2BQ by DAF/Pd(OAc)₂ to form tBuBQ and [Pd^I(μ-DAF)(OAc)]₂. Reaction conditions: [Pd(OAc)₂] = 13.5 mM; [DAF] = 13.5 mM; [tBuH_2BQ] = 6.75 mM. B: Reverse Reaction: oxidation of [Pd^I(μ-DAF)(OAc)]₂ by tBuBQ to form tBuH_2BQ and DAF/Pd(OAc)₂. [Pd^I(μ-DAF)(OAc)]₂ = 6.75 mM; [tBuBQ] = 6.75 mM. C. Linear free energy relationship of log(K_{eq}) $E_{Q/H2Q}$ (dioxane/AcOH). Reaction conditions: [DAF] = 13.5 mM; [Pd(OAc)₂] = 13.5 mM; [H₂Q] = variable (see Supporting Information sections 3 and 4 for details).

Similar data were then obtained with a series of other hydroquinone derivatives in their reaction with DAF/Pd(OAc)₂ in dioxane/AcOD- d_4 , with the equilibrium concentrations of species analyzed by ¹H NMR spectroscopy. The equilibrium constants obtained from these experiments follow a logical trend, with more electron-rich hydroquinones exhibiting higher equilibrium constants: 2,6-Me2H₂BQ ($K_{eq} = 7241$ M), $t_{eq} = 305$ M; see above), MeH₂BQ, ($K_{eq} = 90$ M), H₂BQ ($K_{eq} = 1$ M) and ClH₂BQ ($K_{eq} = 0.4$ M). One-electron and 2H⁺/2e⁻ redox potentials for these quinones have been reported in the literature; however, the values were obtained under different conditions. ⁵⁹ Efforts to obtain potentials under the present reaction conditions were complicated by irreversible cyclic voltammograms, but reliable values could be obtained by

performing open circuit potential measurements with 1:1 mixtures of the corresponding hydroquinone/benzoquinone species. 60 Reduction potentials determined by this method, designated $E_{Q/H2Q}$ (dioxane/AcOH), are as follows: 2,6-Me₂BQ: -109 mV, $^{\prime}$ BuBQ: -67 mV, MeBQ: -43 mV, BQ: 4 mV, ClBQ: 36 mV, all referenced to Fc^{+/0} (see section 6 of the Supporting Information for details). A plot of $\log(K_{eq})$ versus $E_{Q/H2Q}$ (dioxane/AcOH) for the different quinones exhibits a linear correlation with a negative slope, reflecting the larger K_{eq} values for quinones with lower redox potentials (Figure 3C). [Nomenclature note: The abbreviation "Q/H₂Q" is used when referring generically to (hydro)quinone species, while "BQ/H₂BQ" specifically refers to the unsubstituted 1,4-(hydro)benzoquinone derivatives.]

Characterization of redox equilibria between (bc)Pd(OAc)₂ and hydroquinones. The well behaved reaction between tBuH_2BQ and (bc)Pd(OAc)₂ was also monitored by tH NMR spectroscopy, and an equilibrium mixture of (bc)Pd(OAc)₂, tBuH_2BQ , and (bc)Pd(tBuBQ) was obtained. Analysis of the reverse reaction, starting with (bc)Pd(tBuBQ) in the presence of AcOD- d_4 cosolvent, led to the same equilibrium mixture (Figures 4A and 4B).

Similar behavior was observed when the reactions were conducted with other hydroquinones. An exception was observed in the reaction of (bc)Pd(OAc)₂ with 2,6-Me₂H₂BQ, which generated substantial amounts of Pd black, probably reflecting the comparative instability of the Pd⁰ complex of the 2,6-disubstituted quinone. For the other four quinones, equilibrium constants were determined according to the expression in eq 3, with the following values: 'BuH₂BQ ($K_{eq} = 129$ M), MeH₂BQ, ($K_{eq} = 30$ M), H₂BQ ($K_{eq} = 3$ M) and ClH₂BQ ($K_{eq} = 0.5$ M).

$$K_{\text{eq}} = \frac{[(\text{bc})\text{Pd}(\text{RBQ})] \cdot [\text{AcOH}]^2}{[(\text{bc})\text{Pd}(\text{OAc})_2] \cdot [\text{RH}_2\text{BQ}]}$$
(3)

The 2H⁺/2e⁻ Q/H₂Q redox potentials were re-determined in this different solvent system via open circuit potential measurements, as described above (see section 6 in the Supporting

Information for details). The values differ slightly (16-31 mV lower) from those measured in dioxane: ${}^{\prime}BuBQ = -98$ mV, MeBQ = -74 mV, BQ = -13 mV, and ClBQ = 10 mV vs. Fc^{+/0}. The plot of log(K_{eq}) versus $E_{Q/H2Q}(CHCl_3/AcOH)$ for the different quinones again exhibits a linear correlation with a negative slope, reflecting larger K_{eq} values for quinones with lower redox potentials (Figure 4C). The somewhat smaller slope of this plot, relative to that in Figure 3C, may be rationalized by enhanced stability of the Pd⁰ complexes with more electron-deficient quinones, which will partially offset the more favorable oxidation of more electron-rich hydroquinones.

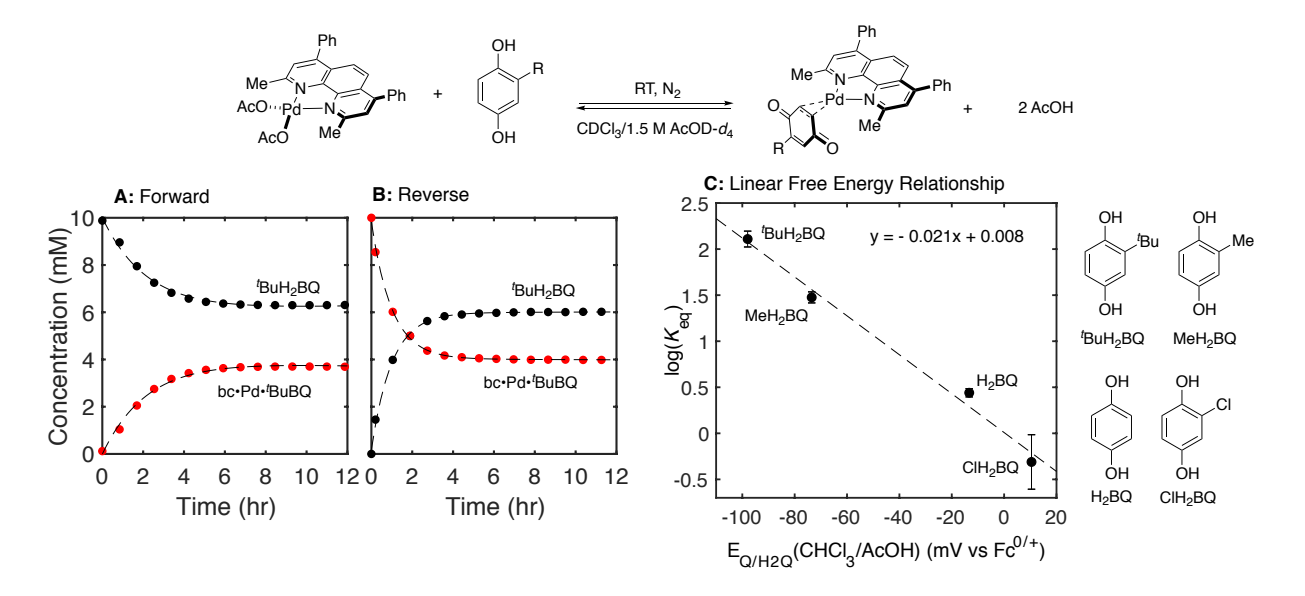


Figure 4. Equilibrium reaction of (bc)Pd(OAc)/BuH₂BQ and (bc)Pd('BuBQ). Reaction conditions: A: Forward): $[(bc)Pd(OAc)_2] = 10.0$ mM; $['BuH_2BQ] = 10.0$ mM. B: Reverse: [(bc)Pd('BuBQ)] = 10 mM C. Linear free energy relationship of $log(K_{eq})$ and $E_{Q/H2Q}(CHCl_3/AcOH)$. Reaction conditions: $[(bc)Pd(OAc)_2] = 10.0$ mM $[H_2Q] = variable$ (see sections 3 and 4 of the Supporting Information for details).

Quantitative Analysis of Ligand Effects on Palladium(II) Reduction Potentials. These well-behaved redox equilibria provide unique access to quantitative ligand effects on Pd^{II} reduction potentials. With DAF as the ancillary ligand, the Q/H_2Q reduction potentials and Pd^{II}/Pd^{I} redox equilibria with different (hydro)quinones may be used to create thermodynamic cycles that allow determination the $2H^+/2e^-$ reduction potential associated with the conversion of 2

DAF/Pd(OAc)₂ into [Pd^I(μ -DAF)(OAc)]₂ + 2 AcOH. The analysis depicted in Scheme 2A shows a thermodynamic cycle using 'BuH₂BQ/'BuBQ as representative (hydro)quinone reagents. The Pd^{II/I} potential is obtained by adding the free energy (ΔG) values from the reaction of DAF/Pd^{II}(OAc)₂ and 'BuH₂BQ and the 'BuBQ/'BuH₂BQ reduction potential, followed by conversion of ΔG into ΔE using the Nernst equation. Similar analysis of the reactions with all five (hydro)quinone derivative led to an average $E_{Pd(II)/Pd(I)}$ value of 12 ± 7 mV vs Fc^{+/0}. We note that the $E_{Pd(II)/Pd(I)}$ value could also be obtained from the linear free energy correlation in Figure 2, by identifying the Q/H₂Q potential corresponding to $\log(K_{eq}) = 0$. The value of $E_{Pd(II)/Pd(I)} = 17$ mV obtained by this approach is within experimental error of the result obtained in Scheme 2A.

Determination of the reduction potential of (bc)Pd(OAc)₂ is a bit more complex due to coordination of the quinone to Pd⁰. The lack of free quinone as a product results in an undefined quinone/hydroquinone redox potential; however, this issue may be addressed by including an additional quinone-exchange equilibrium at Pd⁰ (c.f. Scheme 2Bii). The latter reaction allows a thermodynamic cycle to be created for determination of the $2H^+/2e^-$ reduction potential of (bc)Pd(OAc)₂/BQ to (bc)Pd⁰(BQ) + 2 AcOH. To complete this analysis, equilibrium constants were measured for the exchange of different quinones at the (bc)Pd⁰ fragment (see section 5 in the Supporting Information for details).^{56, 61} A representative thermodynamic cycle, using the equilibrium exchange of BQ and 'BuBQ at Pd⁰ and 'BuH₂BQ/'BuBQ as a reference redox couple, is depicted in Scheme 2B. The reaction free energies may be summed, and the resulting ΔG value may then be used to obtain the $E_{Pd(\Pi)/Pd(0)}$ value. Use of four different reference Q/H₂Q potentials and Pd⁰-BQ/Q exchange equilibrium constants led to an average value of $E_{Pd(\Pi)/Pd(0)} = -4 \pm 18$ mV vs Fc^{+/0}.

Scheme 2. Determination of $(L)Pd(OAc)_2$ Reduction Potentials in Dioxane/AcOH (L = DAF) and $CHCl_3/AcOH$ (L = bc)

A. Thermodynamic Cycle for Determination of DAF/Pd(OAc)₂ Reduction Potential in dioxane/AcOD-d₄

(iii)
$$2 \text{ DAF/Pd}(\text{OAc})_2 + 2 \text{ H}^+ + 2 \text{ e}^ O + 2 \text{ AcOH}$$
 $E_{\text{Pd}(II)/\text{Pd}(I)} = 7 \text{ mV (vs Fc}^{+/0})$

Quinone	K_{rxn} (M)	$E_{\rm Q/H2Q}~({\rm mV~vs~Fc^{+/0}})$	$E_{Pd(II)/Pd(I)}$ (mV vs Fc	· ^{+/0})
2,6-Me ₂ BQ	7241	-109	6	
^t BuBQ	305	-67	7	average
MeBQ	90	-43	14	
BQ	1	4	9	$E_{Pd(II)/Pd(I)} = 12 \pm 7 \text{ mV}$ vs Fc ^{+/0}
CIBQ	0.4	36	23	

B. Thermodynamic Cycle for Determination of (bc)Pd(OAc)₂ Reduction Potential In CDCl₃/1.5 M AcOD-d₄

(iv)
$$\begin{array}{c} Ph \\ + 2 H^{+} + 2 e^{-} \\ + AcO \\ Me \end{array}$$
 $\begin{array}{c} Ph \\ + 2 H^{+} + 2 e^{-} \\ + AcO \\ Me \end{array}$ $\begin{array}{c} Ph \\ + 2 AcOH \\ - Pd \\$

Quinone	K_{rxn}	$K_{ m exchange}$	$E_{\rm Q/H2Q}$ (mV vs Fc ^{+/0})	$E_{Pd(II)/Pd(0)}$ (mV vs	Fc ^{+/0})
^t BuBQ	129	39	-98	12	
MeBQ	30	12	-74	2	average
BQ	3	1	-13	-0.3	$E_{Pd(II)/Pd(0)} = -4 \pm 18 \text{ mV}$ vs Fc ^{+/0}
CIBQ	0.5	0.1	10	-29	V310

DFT Computational Analysis of Ligand Effects on Pd^{II/0} Reduction Potentials. Palladium/quinone redox equilibria were not experimentally accessible for all of the ligands in Figure 1 due to complications arising from poor solubility and/or instability of the Pd⁰-quinone complexes. To address these cases, density functional theory (DFT) calculations were employed, using experimental data for the DAF- and bc-ligated Pd(OAc)₂ complexes as benchmarks. These calculations were conducted at the B3LYP-D3(BJ)/[6-31G(d,p) + Lanl2dz (Pd)] level of theory, with the corresponding Hay-Wadt effective core potential for Pd. Bulk solvent effects were incorporated at the IEF-PCM level (chloroform, $\varepsilon = 4.7113$). $^{62-71}$ The calculated thermodynamic data are reported at a temperature of 298.15 K.

DFT data were used to analyze the thermodynamics for oxidation of H_2BQ by the different (L)Pd(OAc)₂ complexes (1) for L = phen, bpy, py, dmphen, dmbpy, and DAF, leading to the formation of (L)Pd⁰(BQ) complexes (2). Initial calculations probed the free energies of ligand exchange for the reaction of different ligands with (phen)Pd(OAc)₂ (ΔG_L ; Figure 5A-*i*). The resulting values show that the different ancillary ligands can lead to substantial changes in the relative stability the (L)Pd(OAc)₂ complexes. Each of these complexes was then used to calculate the reaction free energy for oxidation of H_2BQ to afford (L)Pd⁰(BQ) and 2 equiv of AcOH (ΔG_{TXR} , Figure 5A-*ii*). This reaction is endergonic for L = py, bpy, and phen, with calculated free energies of the reactions of $\Delta G_{TXR} = +10.6$, +6.0, and +3.9 kcal/mol, respectively. The reaction of H_2BQ with (L)Pd(OAc)₂ complexes with L = dmbpy, dmphen and DAF are exergonic, with $\Delta G_{TXR} = -0.7$, -2.7, and -4.5 kcal/mol, respectively. We also computed the free energy for the reaction of 2 (DAF)Pd(OAc)₂ with H_2BQ to generate [Pd¹(μ -DAF)(OAc)]₂ and free BQ. This reaction proved to be even more exergonic than formation of the (DAF)Pd⁰(BQ) adduct ($\Delta G = -6.7$ kcal/mol; Figure 5A - gray reaction in energy diagram), consistent with experimentally observed formation

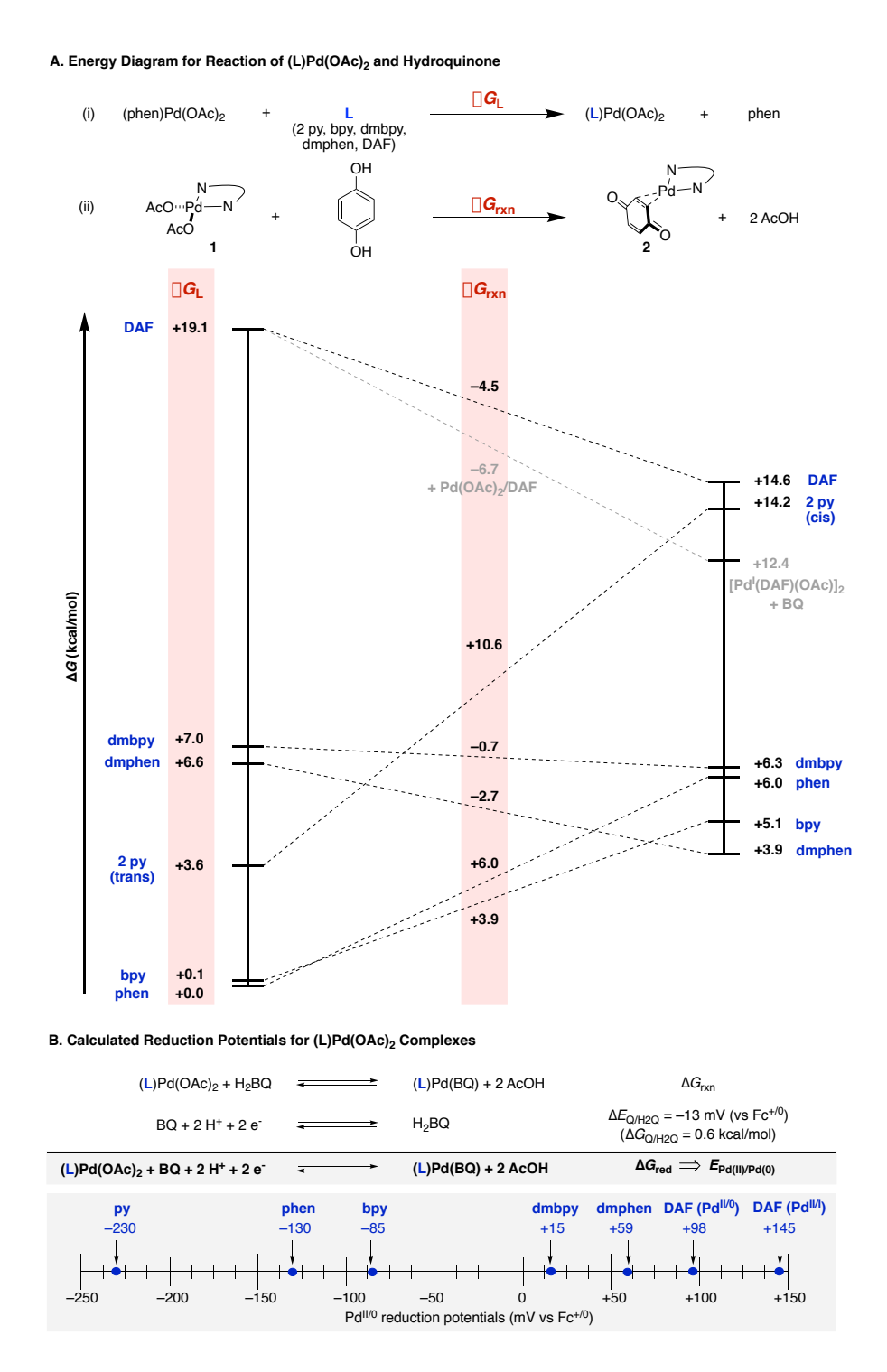


Figure 5. A. Energy diagram for reaction of (L)Pd(OAc)₂ and hydroquinone. Energies of (L)Pd(OAc)₂ complexes are reported relative to (phen)Pd(OAc)₂. B. Scale showing calculated reduction potentials for (L)Pd(OAc)₂ complexes.

of the Pd^I dimer, rather than a (DAF)Pd⁰-BQ adduct. More broadly, these results show good qualitative alignment with the experimental ligand effects on the reaction of Pd(OAc)₂ with $^{\prime}$ BuH₂BQ CHCl₃/AcOD- $^{\prime}$ d₄, (cf. Figure 2) in which little or no reaction was observed with L = py, bpy, and phen, while $^{\prime}$ BuH₂BQ oxidation was observed with L = dmbpy, dmphen, and DAF.

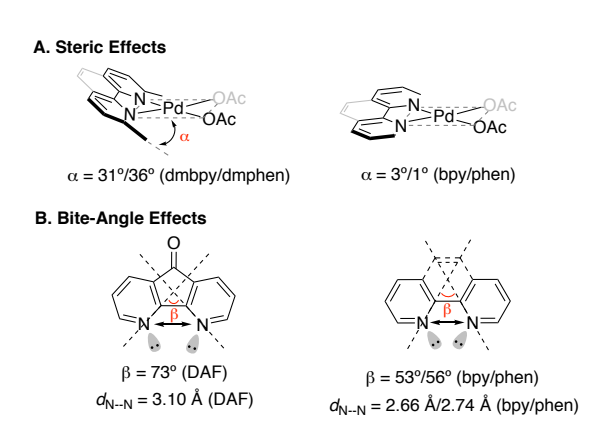
Ligand-based differences in energies are more significant for the Pd^{II} complexes than the Pd^0 complexes. This behavior is evident, for example, from the effect of adding methyl groups adjacent to nitrogen in the bpy and phen ligands. The $(L)Pd(OAc)_2$ complexes with L = dmbpy and dmphen, are approximately 7 kcal/mol higher in energy than the analogs with L = bpy and phen, while the corresponding $(L)Pd^0(BQ)$ complexes for L = bpy, phen, dmbpy and dmphen span a range of energies of only 2.4 kcal/mol, with the dmphen complex having the lowest energy. Pyridine has intermediate stability among the different non-DAF ligands but leads to a particularly unstable $Pd^0(BQ)$ complex.

The calculated $\Delta G_{\rm rxn}$ values (see Figure 5A-*i*) together with the experimental 2H⁺/2e⁻BQ/H₂BQ reduction potential (-13 mV vs Fc^{+/0}) may be used to determine reduction potentials for each of the (L)Pd(OAc)₂ complexes, resembling the approach illustrated in Scheme 2B. The results reveal that the ligands lead to (L)Pd(OAc)₂ reduction potentials that span 375 mV (Figure 5B): L = DAF (to form [Pd^I(DAF)(μ -OAc)]₂): +145 mV; L = DAF (to form (DAF)Pd(BQ)): +98 mV; L = dmphen: +59 mV; L = dmbpy: +15 mV; L = bpy: -85 mV; L = phen: -130 mV; L = py: -230 mV.

Summary and Implications of Ligand Effects on Palladium(II) Reduction Potentials. The above data show that the ancillary ligand can significantly impact the Pd^{II} reduction potential and provide, for the first time, a quantitative assessment of this effect for catalytically relevant Pd complexes. Several specific results warrant further commentary. The methyl groups of the dmbpy

and dmphen ligands increase the Pd^{II} reduction potential by 100 and 189 mV, respectively, relative to the corresponding bpy and phen complexes. This effect rationalizes the ability of dmbpy- and dmphen-ligated Pd(OAc)₂ to promote more favorable oxidation of H₂Q derivatives relative to the bpy- and phen-ligated complexes (cf. Figure 2). This ligand-based increase in redox potential also implicates a thermodynamic contribution to the success of dmbpy and dmphen ligands in Pd-catalyzed aerobic oxidations, including alcohol oxidation,^{43–46} aza-Wacker,²³ and oxidative Heck reactions.^{72–74} The higher energy of the dmbpy- and dmphen-ligated Pd(OAc)₂, relative to the bpy- and phen-ligand complexes, arises from destabilizing steric interactions between the ligand methyl groups and the acetate groups, which distort the coordination geometry of the planar ligand, forcing it out of the Pd^{II} square plane (Scheme 3). This geometrical distortion has been noted in previously reported crystal structures of these complexes;^{23,75,76} however, the work here provides the first insight into the impact of this effect on the Pd^{II} reduction potential.

Scheme 3. Ligand-Based Structure Contributions to Modulation of PdII Reduction Potentials



The thermodynamic influence of DAF is even more profound and especially reflects the destabilization of Pd^{II}, rationalized by distortion of the bite angle of DAF relative to conventional bpy and phen ligands (Scheme 3).^{23,41} Insights from the present study rationalize some of the

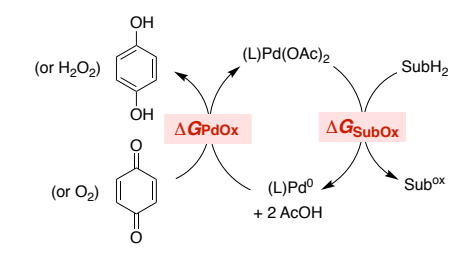
unusual kinetic behavior that has been observed in DAF/Pd(OAc)₂-catalyzed oxidation reactions. For example, aza-Wacker and allylic oxidation exhibit a kinetic burst at the beginning of the reaction when DAF is used as an ancillary ligand.^{42,53} This burst phase arises from stoichiometric substrate oxidation by the DAF/Pd(OAc)₂ species and generates the Pd¹ dimer, [Pd¹(DAF)(μ-OAc)]₂. This burst is followed by a slower steady-state phase of the reaction, and mechanistic data indicate that the steady-state turnover features a more conventional Pd^{11/0} cycle.⁴² The relative rates of the initial burst and steady-state phases of the reaction align the different driving force provided by the Pd^{11/1} vs Pd^{11/0} redox processes, in which the stronger driving force for the Pd^{11/1} process contributes to the more rapid rate.

More generally, the observations here illustrate how ligands may be used to modulate the Pd^{II} reduction potential and thereby impact the driving force for oxidation reactions mediated by palladium(II) (ΔG_{SubOx} , Scheme 4A). The majority of Pd^{II}-catalyzed oxidation reactions feature turnover-limiting steps associated with the substrate oxidation half-reaction (e.g., reductive elimination, transmetalation, β -hydride elimination). R Ligands such as dmbpy, dmphen, and DAF that increase the Pd^{II} reduction potential will provide additional driving force for the net half-reaction, likely promoting faster rates and more effective substrate oxidation. Such benefits will ultimately reach a limit, however, controlled by the thermodynamics of the Pd oxidation half-reaction (ΔG_{PdOx} , Scheme 4A). Benzoquinone has been widely used as an oxidant for this reaction, but the present study reveals that, in some cases, the relative reduction potential of Pd^{II} and BQ can invert, and BQ will not have sufficient driving force for reoxidation of the Pd catalyst. Hints of this behavior are evident in Pd-oxidation reactions that are inhibited by BQ, 77,78 and certain cases in which oxidation of the Pd catalyst is turnover-limiting. Such insights have direct implications for the use of O₂ as an oxidant because the 2H⁺/2e⁻ reduction potential of O₂ to H₂O₂

is virtually identical to that of BQ to H₂BQ (0.68/0.69 V vs NHE, Scheme 4B). This relationship is evident in the nearly isoergic exchange of BQ and O₂ that has been observed at a bc-ligated Pd center (Scheme 4C). ^{79,80} On the other hand, the 4H⁺/4e⁻reduction of O₂ to water provides additional driving force (1.23 V) relative to the 2H⁺/2e⁻ process (Scheme 4B). Mechanisms capable of leveraging this O₂ reduction pathway provide a strategy to expand the scope and utility of Pd-catalyzed aerobic oxidation reactions. ^{81–86}

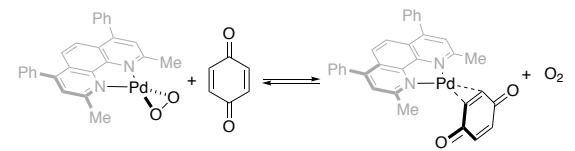
Scheme 4. Thermodynamic Considerations for PdII-Catalyzed Oxidation Reactions

A. Free Energies of Redox Half-Reactions



B. Free Energies of Redox Half-Reactions

C. Quinone/O₂ Exchange Reaction at bc-Ligated Pd Center (ref. 78)



Conclusions. The present study provides unique insights into the influence of ancillary ligands on Pd^{II} reduction potentials, arising from the unexpected discovery that certain ligands enable equilibrium-controlled oxidation of hydroquinone derivatives. Oxidation of hydroquinone by Pd^{II} is opposite to the direction of reactivity usually encountered in Pd-catalyzed oxidation reactions, where BQ is often used as a stoichiometric or co-catalytic reagent to re-oxidize the Pd catalyst. A

noteworthy outcome of this study is the insight that coordination of electron-donating ancillary ligands do not necessarily lower the reduction potential of $Pd(OAc)_2$. Three of the $(L)Pd(OAc)_2$ complexes studied here (L = 2 py, bpy, and phen), in addition to $Pd(OAc)_2$ itself, did not promote oxidation of 4BuH_2BQ , while $(L)Pd(OAc)_2$ complexes with four other ligands (L = dmbpy, dmphen, bc, and DAF) promoted this oxidation reaction. Experimental and computational analysis of the ligand effects show that this series of common nitrogen-based ligands leads to $2H^+/2e^-$ reduction potentials for $(L)Pd(OAc)_2$ complexes that vary by 375 mV, with values falling both above and below the $2H^+/2e^-$ reduction potentials for BQ derivatives.

These results have important implications for further development of Pd-catalyzed oxidation reactions by highlighting the thermodynamic influence of ancillary ligands on the Pd^{II} reduction potential. The insights point to the value of identifying new ligands that destabilize Pd^{II} via steric effects (as with dmbpy, dmphen, and bc) or electronic effects (as with DAF), thereby increasing the driving force for substrate oxidation by Pd^{II}. The results of this study, however, also show that such efforts will need to be complemented by consideration of the oxidant used in the reaction to ensure that both substrate and Pd oxidation half-reactions are favorable and effective.

ASSOCIATED CONTENT

Supporting Information. The Supporting Information is available free of charge on the ACS Publications website: Experimental details and compound characterization data (PDF); X-ray crystallographic data (CIF).

AUTHOR INFORMATION

Corresponding Author

Shannon S. Stahl - Department of Chemistry, University of Wisconsin-Madison, Madison, Wisconsin 53706, United States; orcid.org/0000-0002-9000-7665; Email: stahl@chem.wisc.edu

Authors

David L. Bruns – Department of Chemistry, University of Wisconsin–Madison, Madison, Wisconsin 53706, United States; orcid.org/0000-0003-2455-502X

Djamaladdin G. Musaev – Cherry L. Emerson Center for Scientific Computation, and Department of Chemistry, Emory University, Atlanta, Georgia 30322, United States; orcid.org/0000-0003-1160-6131; Email: dmusaev@emory.edu

Notes

The authors declare no competing financial interests.

ACKNOWLEDGMENT

We benefited from a number of valuable discussions with Josh Buss and Chase Salazar (UW-Madison) and assistance from Ilia Guzei and Amelia Wheaton (UW-Madison) with X-ray diffraction data analysis. Funding for the experimental work was provided by the National Science Foundation (CHE-1665120 and CHE-1953926; SSS), and computational studies were supported by the NSF-CCI Center for C–H Functionalization (CHE-1700982, DGM). Spectroscopic instrumentation was supported by a gift from Paul J. Bender, NSF (CHE1048642), and the NIH (1S10 OD020022-1). DGM gratefully acknowledges the use of resources of the Cherry L. Emerson Center for Scientific Computation (Emory University).

References.

- 1. Smidt, J.; Hafner, W.; Jira, R.; Sedlmeier, J.; Sieber, R.; Rüttinger, R.; Kojer, H. Catalytic Reactions of Olefins on Compounds of the Platinum Group. *Angew. Chem.* **1959**, *71*, 176-182.
- 2. Zeni, G.; Larock, R. C. Synthesis of Heterocycles via Palladium π -Olefin and π -Alkyne Chemistry. *Chem. Rev.* **2004**, *104*, 2285-2309.
- 3. Beccalli, E. M.; Broggini, G.; Martinelli, M.; Sottocornola, S. C-C, C-O, C-N Bond Formation on sp² Carbon by Pd(II)-Catalyzed Reactions Involving Oxidant Agents. *Chem. Rev.* **2007**, *107*, 5318-5365.

- 4. Minatti, A.; Muñiz, K. Intramolecular Aminopalladation of Alkenes as a Key Step to Pyrrolidines and Related Heterocycles. *Chem. Soc. Rev.* **2007**, *36*, 1142-1152.
- McDonald, R. I.; Liu, G. S.; Stahl, S. S. Palladium(II)-Catalyzed Alkene Functionalization via Nucleopalladation: Stereochemical Pathways and Enantioselective Catalytic Applications. *Chem. Rev.* 2011, 111, 2981-3019.
- 6. Bäckvall, J.-E. In *Metal-Catalyzed Cross-Coupling Reactions*, 2nd ed.; de Meijere A., Diederich F., Eds. Wiley-VCH: Weinheim, **2004**; Vol. 2, p 479-529.
- 7. Yeung, C. S.; Dong, V. M. Catalytic Dehydrogenative Cross-Coupling: Forming Carbon-Carbon Bonds by Oxidizing Two Carbon-Hydrogen Bonds. *Chem. Rev.* **2011**, *111*, 1215-1292.
- 8. Liu, C.; Zhang, H.; Shi, W.; Lei, A. Bond Formations between Two Nucleophiles: Transition Metal Catalyzed Oxidative Cross-Coupling Reactions. *Chem. Rev.* **2011**, *111*, 1780-1824.
- 9. Jia, C.; Kitamura, T.; Fujiwara, Y. Catalytic Functionalization of Arenes via C–H Bond Activation. *Acc. Chem. Res.* **2001**, *34*, 633-639.
- Le Bras, J.; Muzart, J. Intermolecular Dehydrogenative Heck Reactions. Chem. Rev. 2011, 111, 1170-1214.
- Liron, F.; Oble, J.; Lorion, M. M.; Poli, G. Direct Allylic Functionalization Through Pd-Catalyzed C-H Activation. *Eur. J. Org. Chem.* 2014, 5863-5883.
- Moiseev, I. I.; Vargaftik, M. N.; Syrkin, Y. K. On the Mechanism of the Reaction of Palladium Salts with Olefins in Hydroxyl-Containing Solutions. *Dokl. Akad. Nauk SSSR* 1960, *133*, 377-380.

- 13. Heumann, Åkermark, B. Oxidation with Palladium Salts: Catalytic Preparation of Allyl Acetates from Monoolefins Using a Three-Component Oxidation System. *Angew. Chem. Int. Ed.* **1984**, *23*, 453-454.
- 14. Bäckvall, J.-E.; Awasthi, A. K.; Renko, Z. D. Biomimetic Aerobic 1,4-Oxidation of 1,3-Dienes Catalyzed by Cobalt Tetraphenylporphyrin-Hydroquinone-Palladium(II). An Example of Triple Catalysis. J. Am. Chem. Soc. 1987, 109, 4750-4752.
- Popp, B. V., Stahl, S. S. Palladium-Catalyzed Oxidation Reactions: Comparison of Benzoquinone and Molecular Oxygen as Stoichiometric Oxidants. *Top. Organomet. Chem.* 2007, 22, 149-189.
- Piera, J.; Bäckvall, J.-E. Catalytic Oxidation of Organic Substrates by Molecular Oxygen and Hydrogen Peroxide by Multistep Electron Transfer—A Biomimetic Approach. *Angew. Chem. Int. Ed.* 2008, 47, 3506-3523.
- Vasseur, A.; Muzart, J.; Le Bras, J. Ubiquitous Benzoquinones, Multitalented Compounds for Palladium-Catalyzed Oxidative Reactions. *Eur. J. Org. Chem.* 2015, 4053-4069.
- 18. Wang, D.; Weinstein, A. B.; White, P. B.; Stahl, S. S. Ligand-Promoted Palladium-Catalyzed Aerobic Oxidation Reactions. *Chem. Rev.* **2018**, *118*, 2636-2679.
- 19. Steinhoff, B. A.; Guzei, I. A.; Stahl, S. S. Mechanistic Characterization of Aerobic Alcohol Oxidation Catalyzed by Pd(OAc)₂/Pyridine Including Identification of the Catalyst Resting State and the Origin of Nonlinear [Catalyst] Dependence. *J. Am. Chem. Soc.* 2004, 126, 11268-11278.

- 20. Schultz, M. J.; Alder, R. S.; Zierkiewicz, W.; Privalov, T.; Sigman, M. S. Using Mechanistic and Computational Studies to Explain Ligand Effects in the Palladium-Catalyzed Aerobic Oxidation of Alcohols. *J. Am. Chem. Soc.* 2005, 127, 8499-8507.
- 21. Zhang, Y.-H.; Shi, B.-F.; Yu, J.-Q. Pd(II)-Catalyzed Olefination of Electron-Deficient Arenes Using 2,6-Dialkylpyridine Ligands. *J. Am. Chem. Soc.* **2009**, *131*, 5072-5074.
- 22. Izawa, Y.; Stahl, S. S. Aerobic Oxidative Coupling of *o*-Xylene: Discovery of 2-Fluoropyridine as a Ligand to Support Selective Pd-Catalyzed C–H Functionalization. *Adv. Synth. Catal.* **2010**, *352*, 3223-3229.
- 23. White, P. B.; Jaworski, J. N.; Zhu, G. H.; Stahl, S. S. Diazafluorenone-Promoted Oxidation Catalysis: Insights into the Role of Bidentate Ligands in Pd-Catalyzed Aerobic Aza-Wacker Reactions. ACS Catal. 2016, 6, 3340-3348.
- 24. Parry, E. P.; Oldham, K. B. Electrochemistry of Palladium(II) Ion in Ammonia and Pyridine Media. *Anal. Chem.* **1968**, *40*, 1031-1036.
- 25. Wan, C. C.; Lai, C. K.; Wang, Y. Y. A Study of the Reduction of Chelated Palladium on Mercury Electrode. *Bull. Chem. Soc. Jpn.* **1991**, *64*, 635-640.
- 26. Azzabi, M., Jutand, A., Amatore, C. Role and Effects of Halide Ions on the Rates and Mechanisms of Oxidative Addition of Iodobenzene to Low-Ligated Zerovalent Palladium Complexes Pd⁰(PPh₃)₂. *J. Am Chem. Soc.* **1991**, *113*, 8375-8384.
- 27. Van Asselt, R., Elsevier, C. J., Jutand, A., Amatore, C. Divalent Palladium and Platinum Complexes Containing Rigid Bidentate Nitrogen Ligands and Electrochemistry of the Palladium Complexes. *Organometallics*. **1997**, *16*, 317-328.

- 28. A rare case of well-behaved Pd^{II/0} electrochemistry has been reported for tetraphosphine-ligated Pd complexes; however, these complexes are rather different from the catalyst species employed in conventional oxidative and non-oxidative coupling reactions. See: Raebiger, J.W., Miedaner, A., Curtis, C.J., Miller, S.M., Anderson, O.P., DuBois, D.L. Using Ligand Bite Angles to Control the Hydricity of Palladium Diphosphine Complexes. *J. Am. Chem. Soc.* **2004**, *126*, 5502-5514.
- 29. Campbell, A.N., White, P. B., Guzei, Ilia, A. G., Stahl, S.S. Allylic C–H Acetoxylation with 4,5-diazafluorenone-Ligated Palladium Catalyst: A Ligand-Based Strategy to Achieve Aerobic Catalytic Turnover. *J. Am. Chem. Soc.* **2010**, *132*, 15116-15119.
- 30. Campbell, A. N.; Meyer, E. B.; Stahl, S. S. Regiocontrolled Aerobic Oxidative Coupling of Indoles and Benzene Using Pd Catalysts with 4,5-Diazafluorene Ligands. *Chem. Commun.* 2011, 47, 10257-10259.
- 31. Xiao, B.; Gong, T.-J.; Liu, Z.-J.; Liu, J.-H.; Luo, D.-F.; Xu, J.; Liu, L. Synthesis of Dibenzofurans via Palladium-Catalyzed Phenol-Directed C–H Activation/C–O Cyclization. *J. Am. Chem. Soc.* **2011**, *133*, 9250-9253.
- 32. Gao, W.; He, Z. Q.; Qian, Y.; Zhao, J.; Huang, Y. General Palladium-Catalyzed Aerobic Dehydrogenation to Generate Double Bonds. *Chem. Sci.* **2012**, *3*, 883-886.
- 33. Diao, T.; Wadzinski, T. J.; Stahl, S. S. Direct Aerobic α,β–Dehydrogenation of Aldehydes and Ketones with a Pd(TFA)2/4,5- Diazafluorenone Catalyst. *Chem. Sci.* **2012**, *3*, 887-891.
- 34. Piotrowicz, M.; Zakrzewski, J. Aerobic Dehydrogenative Heck Reaction of Ferrocene with a Pd(OAc)2/4,5-Diazafluoren-9-one Catalyst. *Organometallics* **2013**, *32*, 5709-5712.

- 35. Buter, J.; Moezelaar, R.; Minnaard, A. J. Enantioselective Palladium Catalyzed Conjugate Additions of Ortho-Substituted Arylboronic Acids to β,β-Disubstituted Cyclic Enones: Total Synthesis of Herbertenediol, Enokipodin A and Enokipodin B. *Org. Biomol. Chem.* **2014**, *12*, 5883-5890.
- 36. Piotrowicz, M.; Zakrzewski, J.; Métivier, R.; Brosseau, A.; Makal, A.; Wózniak, K. Aerobic Palladium(II)-Catalyzed Dehydrogenative Heck Reaction in the Synthesis of Pyrenyl Fluorophores. A Photophysical Study of β-Pyrenyl Acrylates in Solution and in the Solid State. *J. Org. Chem.* **2015**, *80*, 2573-2581.
- 37. Vasseur, A.; Laugel, C.; Harakat, D.; Muzart, J.; Le Bras, J. Ligand-Promoted Reactivity of Alkenes in Dehydrogenative Heck Reactions of Furans and Thiophenes. *Eur. J. Org. Chem.* 2015, 5, 944-948.
- 38. Kim, H. T.; Ha, H.; Kang, G.; Kim, O. S.; Ryu, H.; Biswas, A. K.; Lim, S. M.; Baik, M.-H.; Joo, J. M. Ligand-Controlled Regiodivergent C-H Alkenylation of Pyrazoles and its Application to the Synthesis of Indazoles. *Angew. Chem. Int. Ed.* **2017**, *56*, 16262-16266.
- 39. Kim, T. H.; Lee, W.; Kim, E.; Joo, J. M. C–H Alkenylation of Pyrroles by Electronically Matching Ligand Control. *Chem. Asian. J.* **2018**, *13*, 2418-2422.
- 40. Zheng, Y.; Xiao, L.; Xie, Q.; Shao, L. Palladium-Catalyzed Synthesis of β,β-Diaryl α,β-Unsaturated Ketones. *Synthesis* **2019**, *51*, 1455-1465.
- 41. White, P. B.; Jaworski, J. N.; Fry, C. G.; Dolinar, B. S.; Guzei, I. A.; Stahl, S. S. Structurally Diverse Diazafluorene-Ligated Palladium(II) Complexes and Their Implications for Aerobic Oxidation Reactions. *J. Am. Chem. Soc.* **2016**, *138*, 4869-4880.

- Jaworski, J. N.; Kozack, C. V.; Tereniak, S. J.; Knapp, S. M.; Landis, C. R.; Miller, J. T.; Stahl,
 S. Operando Spectroscopic and Kinetic Characterization of Aerobic Allylic C–H
 Acetoxylation Catalyzed by Pd(OAc)2/4,5-Diazafluoren-9- one. *J. Am. Chem. Soc.* 2019, 141, 10462-10474.
- 43. ten Brink, G. J.; Arends, I. W. C. E.; Hoogenraad, M.; Verspui, G.; Sheldon, R. A. Catalytic Conversions in Water. Part 23: Steric Effects and Increased Substrate Scope in the Palladium-Neocuproine Catalyzed Aerobic Oxidation of Alcohols in Aqueous Solvents. *Adv. Synth. Catal.* **2003**, *345*, 1341-1352.
- 44. Conley, N. R.; Labios, L. A.; Pearson, D. M.; McCrory, C. C. L.; Waymouth, R. M. Aerobic Alcohol Oxidation with Cationic Palladium Complexes: Insights into Catalyst Design and Decomposition. *Organometallics* **2007**, *26*, 5447-5453.
- 45. Painter, R. M.; Pearson, D. M.; Waymouth, R. M. Selective Catalytic Oxidation of Glycerol to Dihydroxyacetone. *Angew. Chem. Int. Ed.* **2010**, *49*, 9456-9459.
- 46. Chung, K.; Banik, S. M.; De Crisci, A. G.; Pearson, D. M.; Blake, T. R.; Olsson, J. V.; Ingram,
 A. J.; Zare, R. N.; Waymouth, R. M. Chemoselective Pd-Catalyzed Oxidation of Polyols:
 Synthetic Scope and Mechanistic Studies. *J. Am. Chem. Soc.* 2013, 135, 7593-7602.
- 47. Kozack, C. V.; Sowin, J. A.; Jaworski, J. N.; Iosub, A. V.; Stahl, S. S. Aerobic Acyloxylation of Allylic C–H Bonds Initiated by a Pd(0) Precatalyst with 4,5-Diazafluoren-9-one as an Ancillary Ligand. *ChemSusChem* **2019**, *12*, 3003-3007.
- 48. Rispoli, P. L.; Coe, J. S. Kinetics of the Oxidation of Benzene-1,4,-Diol by Palladium(II) Compounds in Aqueous Solution. *Dalton. Trans.* **1976**, 2215-2218.

- 49. Toshikazu, H.; Toshihide, M.; Mitsuru, O.; Yoshiki, O. Redox System of Palladium-Trimethyl Ester of Coenzyme PQQ. *Chem. Lett.* **1989**, *18*, 785-786.
- 50. Toshikazu, H.; Toshihide, M.; Mitsuru, O.; Yoshiki, O. Trimethyl Ester of Coenzyme PQQ in Redox Reactions with Transition Metals. An Efficient System for the Palladium-Catalyzed Ring-Opening Reaction of α,β-Epoxysilane *Chem. Lett.* **1991**, *20*, 299-302.
- 51. Zheng, B.; Schmidt, M. A.; Eastgate, M. D. Synergistic Catalysis: Pd(II) Catalyzed Oxidation of 1,4-Dihydroquinones in the Pd(II) Catalyzed 1,4-Oxidation of Cyclic 1,3-Dienes. *J. Org. Chem.* **2016**, *81*, 3112-3118.
- 52. Horak, K. T.; Agapie, T. Dioxygen Reduction by a Pd(0)-Hydroquinone Diphosphine Complex. *J. Am. Chem. Soc.* **2016**, *138*, 3443-3452.
- 53. Jaworski, J. N.; McCann, S. D.; Guzei, I. A.; Stahl, S. S. Detection of Palladium(I) in Aerobic Oxidation Catalysis. *Angew. Chem. Int. Ed.* **2017**, *56*, 3605-3610.
- 54. Milani, B.; Anzilutti, A.; Vicentini, L.; Sessanta o Santi, A.; Zangrando, E.; Geremia, S.; Mestroni, G. Bis-Chelated Palladium(II) Complexes with Nitrogen-Donor Chelating Ligands are Efficient Catalyst Precursors for the CO/Styrene Copolymerization Reaction.

 Organometallics. 1997, 16, 5064-5075.
- 55. Klein, R. A.; Witte, P.; van Belzen, R.; Fraanje, J.; Goubitz, K.; Numan, M.; Schenk, H.; Ernisting, J. M.; Elsevier, C. J. Monodentate and Bridging Coordination of 3,3'-Annelated 2,2'-Bipyridines in Zerovalent Palladium- and Platinum-*p*-Quinone Complexes. *Eur. J. Inorg. Chem.* **1998**, 319-330.
- 56. Canovese, L.; Visentin, F.; Chessa, G.; Uguagliati, P.; Dolmella, A. Synthesis, Characterization and X-Ray Structural Determination of Palladium(0)–Olefin Complexes

- Containing Pyridine-Thioethers Ancillary Ligands. Equilibria and Rates of Olefin and Ligand Exchange. *J. Organomet. Chem.* **2000**, *601*, 1-15.
- 57. Canovese, L.; Visentin, F. Synthesis, Stability and Reactivity of Palladium(0)–Olefin Complexes Bearing Labile or Hemi-Labile Ancillary Ligands and Electron-poor Olefins. *Inorg. Chim. Acta.* **2010**, *363*, 2375-2386.
- 58. Canovese, L.; Visentin, F.; Santo, C.; Bertolasi, V. Low Valent Palladium Benzoquinone Complexes Bearing Different Spectator Ligands. The Versatile Coordinative Capability of Benzoquinone. *J. Organomet. Chem.* **2014**, *749*, 379-386.
- 59. Huynh, M. T.; Anson, C. W.; Cavell, A. C.; Stahl, S. S.; Hammes-Schiffer, S. Quinone 1 e⁻ and 2 e⁻/2 H⁺ Reduction Potentials: Identification and Analysis of Deviations from Systematic Scaling Relationships. *J. Am. Chem. Soc.* **2016**, *138*, 15903-15910.
- 60. A systematic presentation of this methodology was recently reported: Wise, C. F.; Agarwal,
 R. G.; Mayer, J. M. Determining Proton-Coupled Standard Potentials and X-H Bond
 Dissociation Free Energies in Nonaqueous Solvents Using Open-Circuit Potential
 Measurements J. Am Chem Soc. 2020, 142, 10681-10691.
- 61. Van Asselt, R.; Elsevier, C. J.; Zerovalent Palladium and Platinum Complexes Containing Rigid Bidentate Nitrogen Ligands and Alkenes: Synthesis, Characterization, Alkene Rotation and Substitution Reactions/X-ray Crystal Structure of [Bis((2,6-diisopropylphenyl)imino)-acenaphthene](maleic anhydride)palladium(0). *Inorg. Chem.* **1994**, *33*, 1521-1531.
- 62. Frisch, M. J.; Trucks, G. W.; Schlegel, H. B.; Scuseria, G. E.; Robb, M. A.; Cheeseman, J. R.; Scalmani, G.; Barone, V.; Mennucci, B.; Petersson, G. A.; Nakatsuji, H.; Caricato, M.; Li, X.; Hratchian, H. P.; Izmaylov, A. F.; Bloino, J.; Zheng, G.; Sonnenberg, J. L.; Hada, M.; Ehara,

M.; Toyota, K.; Fukuda, R.; Hasegawa, J.; Ishida, M.; Nakajima, T.; Honda, Y.; Kitao, O.; Nakai, H.; Vreven, T.; Montgomery, J. A., Jr.; Peralta, J. E.; Ogliaro, F.; Bearpark, M.; Heyd, J. J.; Brothers, E.; Kudin, K. N.; Staroverov, V. N.; Kobayashi, R.; Normand, J.; Raghavachari, K.; Rendell, A.; Burant, J. C.; Iyengar, S. S.; Tomasi, J.; Cossi, M.; Rega, N.; Millam, M. J.; Klene, M.; Knox, J. E.; Cross, J. B.; Bakken, V.; Adamo, C.; Jaramillo, J.; Gomperts, R.; Stratmann, R. E.; Yazyev, O.; Austin, A. J.; Cammi, R.; Pomelli, C.; Ochterski, J. W.; Martin, R. L.; Morokuma, K.; Zakrzewski, V. G.; Voth, G. A.; Salvador, P.; Dannenberg, J. J.; Dapprich, S.; Daniels, A. D.; Farkas, Ö.; Foresman, J. B.; Ortiz, J. V.; Cioslowski, J.; Fox, D. J., *Gaussian 09, Revision D.01*, Gaussian, Inc., Wallingford CT, **2009**.

- 63. Hay, P. J.; Wadt, W. R. Ab Initio Effective Core potentials for Molecular Calculations. Potentials for the Transition Metal Atoms Sc to Hg. *J. Chem. Phys.* **1985**, *82*, 270-283.
- 64. Wadt, W. R.; Hay, P. J. Ab Initio Effective Core Potentials for Molecular Calculations. Potentials for Main Group Elements Na to Bi. *J. Chem. Phys.* **1985**, *82*, 284-298.
- 65. Becke, A. D. Density-functional Exchange-energy Approximation with Correct Asymptotic Behavior. *Phys. Rev. A* **1988**, *38*, 3098-3100.
- 66. Lee, C.; Yang, W.; Parr, R. G. Development of the Colle-Salvetti Correlation-energy Formula into a Functional of the Electron Density. *Phys. Rev. B* **1988**, *37*, 785-789.
- 67. Becke, A. D. A New Mixing of Hartree–Fock and Local Density Functional Theories. *J. Chem. Phys.* **1993**, *98*, 1372-1377.
- 68. Grimme, S.; Antony, J.; Ehrlich, S.; Krieg, H. A Consistent and Accurate Ab Initio Parametrization of Density Functional Dispersion Correction (DFT-D) for the 94 Elements H-Pu. *J. Chem. Phys.* **2010**, *132*, 154104.

- 69. Cancès, E.; Mennucci, B.; Tomasi, J. A New Integral Equation Formalism for the Polarizable Continuum Model: Theoretical Background and Applications to Isotropic and Anisotropic Dielectrics. *J. Chem. Phys.* **1997**, *107*, 3032-3041.
- 70. Mennucci, B.; Tomasi, J. Continuum Solvation Models: A New Approach to the Problem of Solute's Charge Distribution and Cavity Boundaries. *J. Chem. Phys.* **1997**, *106*, 5151-5158.
- 71. Scalmani, G.; Frisch, M. J. Continuous Surface Charge Polarizable Continuum Models of Solvation. I. General Formalism. *J. Chem. Phys.* **2010**, *132*, 114110.
- 72. Andappan, M. M. S.; Nilsson, P.; Larhed, M. The First Ligand-Modulated Oxidative Heck Vinylation. Efficient Catalysis with Molecular Oxygen as Palladium(0) Oxidant. *Chem. Commun.* **2004**, 218-219.
- 73. Lindh, J.; Enquist, P.; Pilotti, Å.; Nilsson, P.; Larhed, M. Efficient Palladium(II) Catalysis under Air. Base-Free Oxidative Heck Reactions at Room Temperature or with Microwave Heating. *J. Org. Chem.* **2007**, *72*, 7957-7962.
- 74. Zheng, C.; Wang, D.; Stahl, S. Catalyst-Controlled Regioselectivity in the Synthesis of Branched Conjugated Dienes via Aerobic Oxidative Heck Reactions. *J. Am. Chem. Soc.* **2012**, *134*, 16496-16499.
- 75. Moulin, S.; Pellerin, O.; Toupet, L.; Paul, F. Formation of Six-membered Palladacycles from Phenanthroline Pd(II) Bisacetate Precursors and Phenylisocyante. *C. R. Chime* **2014**, *17*, 521-525.
- 76. Milani, B.; Alessio, E.; Mestroni, G.; Sommazzi, A.; Garbassi, F.; Zangrando, E.; Bresciani-Pahor, N.; Randaccio, L. Synthesis and Characterization of Monochelated Carboxylatopalladium(II) Complexes with Nitrogen-donor Chelating Ligands. Crystal

- Structures of Diaceto(1,10-phenanthroline)- and Diaceto(2,9-dimethyl-1,10-phenanthroline)- Palladium(II). *J. Chem. Soc. Dalton Trans.* **1994**, 1903-1911.
- 77. Pattillo, C. C.; Strambeanu, I. I.; Calleja, P.; Vermeulen, N. A.; Mizuno, T.; White, M. C. Aerobic Linear Allylic C–H Amination: Overcoming Benzoquinone Inhibition. *J. Am. Chem. Soc.* **2016**, *138*, 1265-1272.
- 78. Salazar, C. A.; Flesch, K. N.; Zhou, P. S.; Musaev, D. G.; Stahl, S. S. Palladium-Catalyzed C—H Oxidative Arylation Accessing High Turnover with O₂. *Submitted for publication*.
- 79. Popp, B. V.; Stahl, S. S. "Oxidatively Induced" Reductive Elimination of Dioxygen from an η²-Peroxopalladium(II) Complex Promoted by Electron-Deficient Alkenes. *J. Am. Chem. Soc.* 2006, 128, 2804-2805.
- 80. Popp, B. V.; Thorman, J. L.; Stahl, S. S. Similarities Between the Reactions of Dioxygen and Alkenes with Palladium(0)- Relevance to the Use of Benzoquinone and Molecular Oxygen as Stoichiometric Oxidants in Palladium-Catalyzed Oxidation Reactions. *J. Mol. Cat. A: Chem.* **2006**, *251*, 2-7.
- 81. Khusnutdinova, J. R.; Rath, P. N; Mirica, L. M. The Aerobic Oxidation of a Pd(II) Dimethyl Complex Leads to Selective Ethane Elimination from at Pd(III) Intermediate. *J. Am. Chem. Soc.* **2012**, *134*, 2414-2422.
- 82. Gerken, J. B.; Stahl, S. S. Similarities High-Potential Electrocatalytic O₂ Reduction with Nitroxyl/NO_x Mediators: Implications for Fuel Cells and Aerobic Oxidation Catalysis. *ACS Cent. Sci.* **2015**, *1*, 234-243.
- 83. Zultanski, S. L..; Stahl, S. S. Palladium-Catalyzed Aerobic Acetoxylation of Benzene Using NO_x-Based Redox Mediators. *J. Organomet. Chem.* **2015**, *793*, 263-268.

- 84. Ingram, A. J.; Walker, K.L; Zare, R. N.; Waymouth, R. M. Catalytic Role of Multinuclear Palladium–Oxygen Intermediates in Aerobic Oxidation Followed by Hydrogen Peroxide Disproportionation. *J. Am. Chem. Soc.* **2015**, *137*, 13632-13646.
- 85. Anson, C. W.; Stahl, S. S. Cooperative Electrocatalytic O₂ Reduction Involving Co(salophen) with *p*-Hydroquinone as an Electron–Proton Transfer Mediator. *J. Am. Chem. Soc.* **2017**, *139*, 18472-18475.
- 86. Maity, A.; Hyun, S.-M.; Powers, D. C. Oxidase Catalysis via Aerobically Generated Hypervalent Iodine Intermediates. *Nat. Chem.* **2018**, *10*, 200-204.

TOC Graphic